Current Opinion in Colloid & Interface Science 36 (2018) 28–36

Contents lists available at ScienceDirect

Current Opinion in Colloid & Interface Science

journal homepage: www.elsevier.com/locate/cocis

Dielectrowetting: The past, present and future

A.M.J. Edwards [a,*], C.V. Brown [a], M.I. Newton [a], G. McHale [b]

[a] School of Science and Technology, Nottingham Trent University, Clifton Lane, Nottingham NG11 8NS, UK
[b] Smart Materials and Surfaces Laboratory, Department of Mathematics, Physics and Electrical Engineering, Northumbria University, Ellison Place, Newcastle upon Tyne NE1 8ST, UK

ARTICLE INFO

Article history:
Received 20 October 2017
Received in revised form 20 November 2017
Accepted 30 November 2017
Available online 20 December 2017

Keywords:
Wetting
Liquid dielectrophoresis
Microfluidics
Optofluidics

ABSTRACT

Liquid dielectrophoresis is a bulk force acting on dipoles within a dielectric liquid inside a non-uniform electric field. When the driving electrodes are interdigitated, bulk liquid dielectrophoresis is converted to an interface-localised form capable of modifying the energy balance at an interface. When the interface is a solid-liquid one, the wetting properties of a surface are modified and this approach is known as dielectrowetting. Dielectrowetting has been shown to provide the ability to reversibly modify the contact angle of a liquid droplet with the application of voltage, the strength of which is controlled by the penetration depth of the non-uniform field and permittivities of the fluids involved. Importantly, dielectrowetting provides the ability to create thin liquid films, overcoming the limitation of contact angle saturation present in electrowetting. In this paper, we review the development of dielectrowetting - its origins, the statics and dynamics of dielectrowetted droplets, and the applications of dielectrowetting in microfluidics and optofluidics. Recent developments in the field are also reviewed showing the future directions of this rapidly developing field.

1. Introduction

The behaviour of liquid droplets on surfaces plays a fundamental role in both domestic and industrial environments; from the application of paint onto a wall to the dispersal of pesticides. Each of these processes benefits from the controllability of the wetting properties of both the surfaces and droplets involved in the system. Thus, the prominence of liquid surface interactions has led to the field of capillarity being one of the largest scientific fields of modern science [1•]. The wetting properties of a surface are often defined by the contact angle θ, which for a droplet in air, is the angle between the liquid-vapor interface and the solid-liquid interface (see Fig. 1). The contact angle is the result of the local minimum in the surface free energy arising from the solid-vapor, solid-liquid and liquid vapor interfaces (γ_{SV}, γ_{SL} and γ_{LV}). This local energy minimum is described by the Young equation:

$$\cos(\theta_Y) = \frac{(\gamma_{SV} - \gamma_{SL})}{\gamma_{LV}} \quad (1)$$

While the equilibrium behaviour of a droplet is defined by Eq. (1), this is only applicable to ideal atomically smooth and chemically heterogeneous surfaces. Real world surfaces are often rough and inhomogeneous chemically, and in these cases the contact angle of a droplet exists between two extremes, the advancing and receding angles. This phenomenon is known as contact angle hysteresis [2] and controls the ability of a droplet to move over the surface. The wetting properties of a surface can be modified through changing the surface chemistry [3] or surface morphology [4], making the surface hydrophilic, hydrophobic, superhydrophilic or superhydrophobic (or olephilic/oleophobic), these changes however are often permanent in nature. Methods to controllably modify the wetting properties of a surface offer many advantages over a permanent modification approach.

There are two methods of modifying the wetting properties of a liquid droplet on a solid surface through electric fields, these are electrowetting and dielectrowetting, both of which are an electrohydrodynamic (EHD) response of a material to an electric field [5]. While electrowetting and dielectrowetting both modify the wetting properties of a liquid droplet on a solid surface through the use of electric fields, the key distinction between the two approaches is that electrowetting occurs through the movement of free charge [6], while dielectrowetting is due to the polarisation of dipoles within the liquid. It has been argued by Jones et al. that when a voltage is applied the electric field near the contact line attracts both free charges as well as the polarised dipoles giving rise to a Maxwell stress on the liquid-air interface which must then decrease the curvature to reduce the Laplace pressure. Therefore, for a conducting liquid, electrowetting and dielectrowetting effects are the low and high frequency responses to an external electric field [7••,8]. In this paper we shall focus our attention onto the behaviour of non-conducting liquid droplets in non-uniform electric fields and as such focus on the dielectrowetting effect, however many reviews can be found on the electrowetting effect [6,9••].

* Corresponding author.
E-mail addresses: andrew.edwards@ntu.ac.uk (A.M.J. Edwards), carl.brown@ntu.ac.uk (C.V. Brown), michael.newton@ntu.ac.uk (M.I. Newton), glen.mchale@northumbria.ac.uk (G. McHale).

https://doi.org/10.1016/j.cocis.2017.11.005
1359-0294/

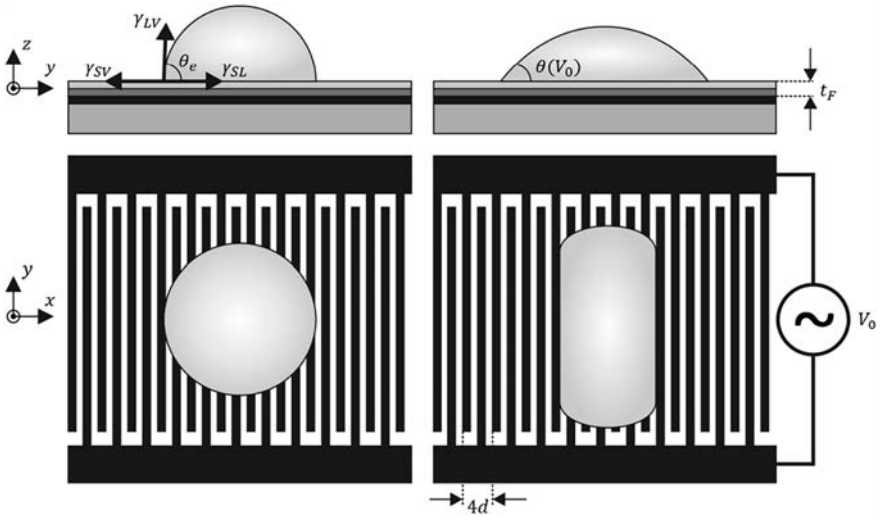

Fig. 1. Schematic of the classic dielectrowetting experiment (in air) showing both before and after voltage is applied between the surface interdigitated electrodes. Not to scale.

Dielectrophoresis refers to the electromechanical force arising from the polarisation of neutral matter in non-uniform electric fields [10]. The key work on the movement of bulk liquids using dielectrophoresis, better known as liquid dielectrophoresis (L-DEP) was performed by Pellat in 1895. He demonstrated the effect of the L-DEP force in increasing the height of rise of a dielectric liquid with a permittivity ε_l between two partially immersed plate electrodes separated by a distance d. With the application of a voltage V, the liquid was observed to rise upward between the plates to a new equilibrium height h given by:

$$h \approx \frac{(\varepsilon_l - \varepsilon_0)}{2\rho g d^2} V^2 \tag{2}$$

where ρ is the density of the liquid, g is the acceleration due to gravity and ε_0 is the permittivity of free space. The L-DEP phenomenon went relatively unexplored until 1971 when Jones et al. developed a dielectric siphon capable of pumping a liquid from a higher reservoir to a lower reservoir when a potential difference of 19 kV is applied between the two plates [11]. They achieved this by raising the liquid to a height at which the hydrostatic pressure creates a flow between the two reservoirs which can be stopped upon removal of the applied voltage. In 2001, Jones and co-workers successfully miniaturised the electrodes used for L-DEP and created a "wall-less" electrode structure capable of moving a dielectric oil up against gravity by several centimetres with only 200 V A.C. [12]. This reduction in voltage stems from the favourable scaling of the L-DEP force with electric field ($F_{DEP} \propto E^2$) [13•,14•].

Following this several groups explored the electrostatic reduction in the contact angle of a droplet using embedded co-planar electrode structures, referred to as co-planar or "contactless" electrowetting, (referring to the removal of the contact wire needed in traditional electrowetting) [15,16]. In these experiments, the contact angle of a de-ionised (DI) water droplet was modified and shown to follow a $\cos(\theta) \propto V^2$ dependence similar to that of electrowetting. Cheng et al. explored the L-DEP effect in modifying the contact angle of a liquid crystal droplet on a surface for the purposes of creating a liquid lens, reporting a recoverable 25° change in contact angle at 200 V [17••]. The first mention of the spreading of a droplet into a thin liquid film through L-DEP on co-planar electrodes was by Brown et al. in 2009, where they spread a droplet of 1-decanol over a surface at $20V_{rms}$ to a uniform thickness of 12 μm, overcoming the contact angle saturation limitation of the electrowetting approach [18••]. This work established the concept of interface-localised liquid dielectrophoresis and used the dielectrophoretic energy to control the shape of the liquid-air interface to create a voltage programmable diffraction grating. This was quickly followed up by McHale et al. in which they elucidated the effect of localizing the L-DEP effect to the solid-liquid interface and derived the relationship between the voltage and contact angle for a dielectric droplet. This was experimentally confirmed by demonstrating a reversible modification of the contact angle of a dielectric droplet from 96° to 23° on non-contacting co-planar electrodes. It was in this paper in which the term "dielectrowetting" was introduced in recognition of the influence of L-DEP in modifying the wetting properties of a liquid on a solid surface [19••].

2. Fundamentals of dielectrowetting

2.1. Static dielectrowetting

To gain a deeper understanding of the dielectrowetting phenomenon, consider a dipole (whether induced or permanent) in a uniform electric field. While the dipole may orientate itself with the electric field there will be no net motion due to the electrostatic forces being equal at each end of the dipole. However, in a non-uniform field the forces at each end of the dipole are not equal and opposite and, due to the higher electric field density at one side, this leads to a net force on the dipole and therefore net motion under the applied electric field. It should be noted here that the charge of the dipole is of little importance because if the field direction is reversed the region of highest electric field remains the same, thus the motion of the dipole is always toward the region of highest electric field. In the dielectrowetting setup interdigitated electrodes (IDE's) are fabricated on or embedded in a solid surface and covered by a dielectric liquid layer of thickness, h. By applying a potential difference V between these IDE's the electric potential of the charged IDE's decays away from the solid surface into the liquid with a penetration depth δ, given by $V(z) = V_0 \exp(-2z/\delta)$.[1] The electrostatic energy per unit contact area stored in the liquid, w_E can then be found by integrating the dielectric energy density, $\frac{1}{2}\varepsilon_0\varepsilon_l \boldsymbol{E}.\boldsymbol{E}$, where ε_m is the dielectric constant of the medium and $\boldsymbol{E} = -\nabla V$ is the electric field,

[1] For linear IDE's having an electrode width and gap of d, the electrical period is $4d$ giving a wave number $k = \pi/2d$. From Poisson's equation, the solution for the potential in a semi-infinite dielectric liquid is of the form ~ $\cos(kx) \times \exp(-kz)$, so the penetration depth is related to the electrode structure by $\delta = 4d/\pi$ [18••,25]. This gives rise to potential energy barriers across the electrodes thus limiting motion to be parallel with the electrode fingers (Fig. 2).

over the volume of the liquid. This leads directly to Eq. (3) [19••,20].

$$w_E = -\frac{\varepsilon_o \varepsilon_m V_0^2}{2\delta}\left[\exp\left(-\frac{4h}{\delta}\right)-1\right] \tag{3}$$

At the limit that the liquid layer is much thicker than the penetration depth of the electric potential ($h \gg \delta$) the energy per unit contact area in the liquid becomes $w_E = \varepsilon_0 \varepsilon_l V_0^2/2\delta$. This means that while L-DEP is a bulk force, in this scenario it is the change in contact area which causes a change in the net dielectrophoretic energy; and the penetration depth of the electric field effectively localises the effect to the vicinity of the solid-liquid interface.

For a dielectric droplet in vapor as the surrounding medium, such that ($h \gg \delta$), the effect of increasing the contact area by a small amount ΔA is to replace the solid-vapor interface by the solid-liquid interface such that the change in free surface energy is $(\gamma_{SL} - \gamma_{SV})\Delta A$, this also creates an additional liquid-vapor surface area of $\Delta A \cos(\theta)$ [21]. In the presence of the non-uniform electric field in the newly expanded region the L-DEP energy changes from its value in the surrounding vapor to that in the liquid, i.e. $-\varepsilon_0(\varepsilon_L - \varepsilon_V)V_0^2\Delta A/2\delta$, where ε_L is the permittivity of the liquid and ε_V is the permittivity of the surrounding vapor. For a droplet to be in local equilibrium the total change in energy must vanish and Eq. (1) becomes:

$$\cos(\theta_e(V_0)) = \cos(\theta_0) + \frac{\varepsilon_0(\varepsilon_L - \varepsilon_V)}{2\gamma_{LV}\delta}V_0^2 \tag{4}$$

Eq. (4) is a modified version of Young's Law, which is also referred to as the "dielectrowetting" equation, similar to the electrowetting equation but where the ratio of the permittivity of the solid insulator to its thickness is replaced by the ratio of the difference in permittivity to the penetration depth of the electric field. Eq. (4) was first deduced by McHale and co-workers in 2011, this paper also experimentally confirmed the relationship between the applied voltage and contact angle using droplets of Propylene Glycol placed on a hydrophobic surface to increase the initial contact angle (Fig. 2) [19••].

Fig. 2 shows the dielectrowetting behaviour of a droplet on linear IDE's, showing that the contact angle decreases with increasing voltage and increases with decreasing voltage; exhibiting only a small degree of contact angle hysteresis which can be attributed to the swapping from advancing to receding angles on the surface. The upper inset of Fig. 2 shows the dependence of $\cos(\theta(V_0))$ on the square of the applied voltage V_0^2 which demonstrates a clear linearity, confirming the relationship

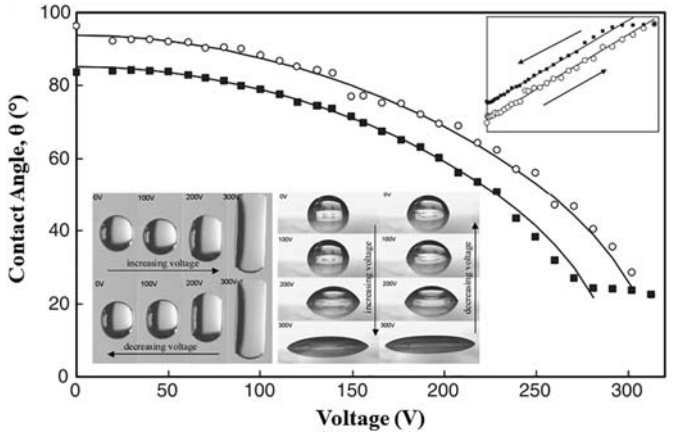

Fig. 2. Control of contact angle for a stripe shaped droplet of 1,2 propylene glycol on a substrate with interdigitated electrodes, hollow circles show increasing voltage half cycle, filled squares show decreasing voltage half cycle. Lower inset shows the top and side views for a range of applied voltages and the upper inset shows the linear fits to the cosine of the contact angle versus voltage squared. Adapted from [22], with the permission of the SPIE.

of Eq. (4). A more accurate form of Eq. (4) should take into account the capacitive division of the applied voltage caused by the inclusion in this experiment of a thin solid dielectric capping layer of thickness t_F, and permittivity, ε_F [19••]. While Eq. (4) predicts an applied voltage at which the contact angle is reduced to zero, a so called threshold voltage for complete wetting V_{th}, this is not achievable experimentally due to the limited area of the electrodes. Instead as $V \to V_{th}$, the liquid spreads to cover the whole of the electrically active area [23•]. In a follow on paper McHale and co-workers then recast Eq. (4) using the value of V_{th}, the voltage at which complete wetting is predicted to occur i.e. $\cos(\theta(V_{th})) = 1$ [24••].

$$\cos(\theta_e(V_0)) = \cos(\theta_0) + [1 - \cos(\theta_0)]\left(\frac{V_0}{V_{th}}\right)^2 \tag{5}$$

This approach combines the electrowetting and dielectrowetting equations into a single unified notational form using two parameters, the initial contact angle, θ_0, and threshold voltage, V_{th}, for complete wetting, which can be determined entirely experimentally through measurement of the contact angle at various applied voltages. In the absence of hysteresis, the initial contact angle, $\theta_0 = \theta(V_0 = 0)$, would be the contact angle given by the Young equation, θ_Y. It should be noted that while the formation of a thin film is possible the contact angle of a droplet can never reach 0° as Eq. (5) is only valid while ($h \gg \delta$) which is not true for fully spread thin films. As the height of the droplet approaches and goes below the penetration depth of the electric field a second regime appears as the electric potential has significant value at the upper surface of the liquid. At which point the liquid-vapor interface can be distorted by the electric field giving rise to surface wrinkles [18•,20,25,26].

2.2. Dynamic dielectrowetting

The static behaviour of liquids on surfaces is not the only important industrial consideration, the speed at which the wetting occurs is also of great consideration, for example when applying the brakes of a car in the rain the thin film of water between the tyre and the road needs to be removed as fast as possible to prevent sliding [27]. In applications such as lab-on-a-chip devices, the dynamics of dielectrowetting governs the response time of the device [28,29]. The speed of a moving contact line is given by a balance between the interfacial forces driving and the viscous forces resisting the motion. This process can be characterised by the dependence of the velocity of the contact line, v_e on the dynamic contact angle $\theta_d(t)$, which often obeys the Hoffman-de Gennes law $v_e \propto \theta(\cos(\theta_0) - \cos(\theta_d(t)))$. For the case of complete wetting of a spherical cap or circular arc cross-sectional shaped droplet of constant volume the time dependence of the dynamic contact angle obeys the simple power law $\theta_d \propto (t + t_0)^n$, where t_0 is a constant and $n = -3/10$ for a spherical cap droplet (Tanner's law) and $n = -2/7$ for a circular cross-section stripe [30,31]. By including the additional energy contribution from the electric field, the Hoffmann-de Gennes law can be modified to include the electric field component of spreading [24••].

$$v_e(t) \approx k\left(\frac{\gamma_{LV}}{\eta}\right)\theta\left[\cos(\theta_0) - \cos(\theta_d(t)) + (1 - \cos(\theta_0))\left(\frac{V}{V_{th}}\right)^2\right] \tag{6}$$

As Eq. (6) is for a spherical cap and classic dielectrowetting experiments produce liquid stripes, by introducing additional geometrical constraints Eq. (6) can be recast, to the first order, to describe a circular

arc cross-section stripe of constant volume, Ω:

$$\frac{d\theta}{dt} \approx -k\left(\frac{\gamma_{LV}}{\eta}\right)\left(\frac{8L_0}{3\Omega}\right)^{\frac{1}{2}}\theta^{\frac{5}{2}}\left[\cos(\theta_0) - \cos(\theta(t)) + (1-\cos(\theta_0))\left(\frac{V}{V_{th}}\right)^2\right] \quad (7)$$

Eq. (7) predicts three regimes, $V \ll V_{th}$, $V \sim V_{th}$ and $V \gg V_{th}$. For $V \ll V_{th}$, the dynamic contact angle is expected to exponentially approach the equilibrium angle with a time constant that changes as a function of the applied voltage such that:

$$\Delta\theta(t) = \Delta\theta_0 \exp\left(-\frac{t}{\tau(V)}\right) \quad (8)$$

where $\tau^{-1} = k(\frac{\gamma_{LV}}{\eta})(\frac{8L_0}{3\Omega})^{\frac{1}{2}}\theta_e^{\frac{7}{2}}(V)$, k is a constant representing the viscous dissipation over the volume of fluid from some microscopic cut-off scale up to a hypothetical boundary within the droplet [1*,21] and $\Delta\theta_0 = \theta(t=0) - \theta_e$ is the constant of integration. As $V \approx V_{th}$ the dynamic contact angle tends to zero in the long time limit and the integration of Eq. (7) gives $\theta \propto (t+t_0)^{-2/7}$, which predicts the dynamic contact angle will decrease following the $-2/7$th power law relationship as reported by McHale and co-workers for dynamic spreading of a stripe, i.e. 2D droplet, on a complete wetting surface [31]. For $V \gg V_{th}$ then the dynamic contact angle still tends to zero at the long time limit however the integration of Eq. (7) results in $\theta \propto (t+t_0)^{-2/3}$ indicating a superspreading behaviour, which can be tuned by the magnitude of the applied voltage. Each of these dynamic behaviours of a dielectrowetted stripe were also experimentally confirmed by McHale et al. (see Fig. 3) [24**]. Thus, dielectrowetting is an approach on par with topography [32] and surfactant driven superspreading [33] while maintaining the ability to recover the initial droplet shape in a voltage programmable manner [34].

2.3. Axisymmetric spreading

While dielectrowetting allows control of the contact angle of a droplet on a solid surface the directional spreading of the droplet is limited by the underlying electrode pattern i.e. droplets spread out parallel to the electrode direction (see Fig. 2). This non-axisymmetric spreading is driven by the electrode fingers acting as potential energy barriers which must be overcome. While concentric circle electrode designs demonstrated by Cheng et al. [17**] allow a dielectrowetted droplet to remain in a spherical cap shape at equilibrium they suffer from quantisation of the contact angle due to the periodic potential barrier problem [35]. To solve the periodic barrier problem Russell and co-workers developed a "zipper" style electrode geometry which has electric field components in both directions [36*]. Using this design, they observed slight axisymmetric spreading however this was limited by the longer supplying parallel electrodes. Russell et al. recently reported achieving omnidirectional spreading using a 500 nm Paralyene C with 50 nm FluoroPel 1601 V dielectric stack [37]. Brabcova et al. recently demonstrated an alternative approach to dielectrowetting using a design consisting of four individually addressable sets of IDE's which was combined with a four phase driving signal [38*]. They suggested that the periodic energy barrier created from the IDE fingers required for dielectrowetting can be overcome through using a multiphase approach (0°, 90°, 180°, 270°), such that the time averaged field provides a spatially uniform electric field in all directions. They experimentally confirmed an improved spreading of a droplet for a given voltage using the four phase approach against the traditional single phase actuation. The partial axisymmetric spreading of a droplet while avoiding the quantisation introduced by using a design based on concentric circular electrodes was also observed due to the spiral type design. Their experiments suggest that in this four phase approach the dependence on the electrode period is changed from a $1/d$ dependence to a $1/d^{0.4}$.

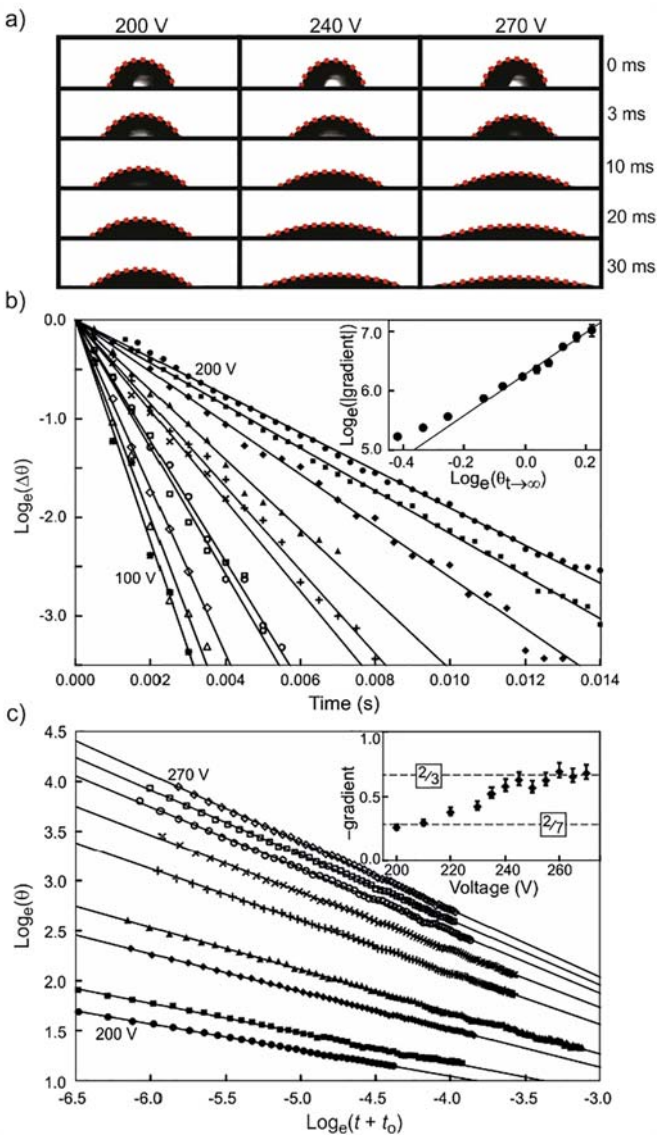

Fig. 3. Dynamical behaviour of a dielectrowetted droplet. (a) Actual droplet shaped profiles as a function of time at 0.87, 1.04 and 1.17V/V_{th} respectively. (b) Exponential approach to equilibrium of dielectrowetted stripes below the threshold voltage. Inset confirms the $\theta_e(V)^{-7/2}$ dependence on the voltage dependent equilibrium contact angle. (c) Power law spreading and superspreading of dielectrowetted stripes showing the dynamic contact angle varies as $\theta \propto 1/(t+t_0)^n$. Inset shows the dependence of n with the spreading voltage showing the transition from 2/7 to 2/3 as the voltage is increased. Graphs & images reproduced from [24**] with permission of the Nature Publishing Group.

2.4. Dielectrowetting in two liquid systems

In the discussion so far we have considered the case of a liquid droplet in a vapor environment being spread through the L-DEP force. However, it is advantageous to work with a two liquid system to reduce actuation voltages, through reduction in contact angle hysteresis, this also has the benefit of creating a neutral buoyancy environment [39–41]. In a two liquid system, the wetting properties of the droplet are dependent on the interfacial tension γ_{LF} between the two fluids, the value of which is typically much lower than the liquid-air surface tension. Returning to Eq. (3), the pre-factor $(\varepsilon_L - \varepsilon_V)$ determines the relative strength of the dielectrowetting component, if the inner liquid is of higher permittivity than the outer i.e. $\varepsilon_L > \varepsilon_V$ then the droplet is spread under the L-DEP force, this is traditional dielectrowetting. However, if $\varepsilon_V > \varepsilon_L$ then the outer liquid will preferentially spread in response to the electric field leading to dewetting of the inner fluid,

this is the reverse of conventional dielectrowetting so called negative liquid dielectrophoresis (nL-DEP) or negative dielectrowetting. Yang et al. explored the wetting behaviour of the nL-DEP effect in 2012 in which they observed a nearly full change of the contact angle from 26° to 176° under the application of 215V_{rms} [35••]. They demonstrated a deviation away from the expected $\cos(\theta) \propto V^2$ behaviour for higher voltages. This deviation could potentially be caused by the deviation from the spherical cap shape at the surface, buoyancy effects, or the underlying non-linear electrode structure (Fig. 4), however this deviation behaviour remains to be fully explained.

Recently Brown et al. developed a theoretical framework for a spreading cuboidal rectangular shaped droplet of volume Ω, in another liquid considering the length and height of the stripe shaped droplet; finding that the height should decrease with the square of the voltage [42].

$$h^2(V_0) = h_0^2 - \frac{\varepsilon_0(\varepsilon_L - \varepsilon_V)\Omega}{4\delta\gamma_{LF}} V_0^2 \tag{9}$$

Eq. (9) was experimentally demonstrated with 5 different liquids in air and several liquid-liquid combinations, showing that liquid-in-liquid dielectrowetting can be a method of determining material properties such as permittivity or interfacial tension from the ratio $\Delta\varepsilon/\gamma_{LF}$. While

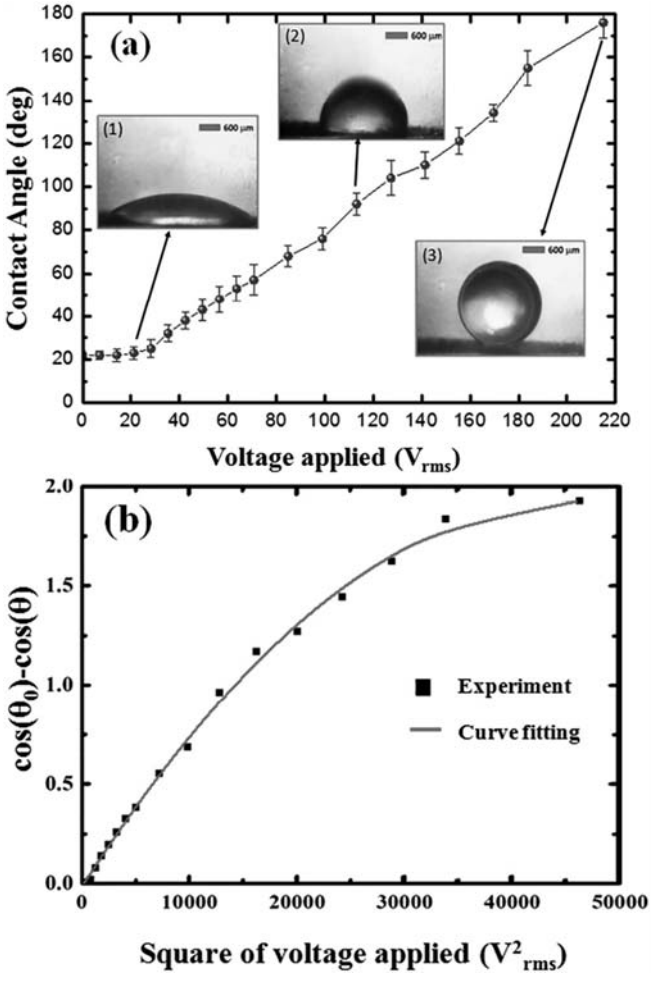

Fig. 4. The behaviour of a silicone oil droplet being displaced through negative dielectrowetting. a) Contact angle as a function of applied voltage (V_{rms}) Inset pictures show the side view of the droplet at applied voltages of 1) 21 V, 2) 113 V and 3) 215 V which correspond to contact angles of 22°, 90° and 176° respectively. b) $cos(\theta_0) - cos(\theta(V))$ plotted against V^2, the solid black line shows a 4th order polynomial fit. Reprinted from [35••], with the permission of AIP Publishing.

the static behaviour of a liquid-in-liquid system is important the operational throughput of any L-DEP based device relies on the dynamical behaviour of the system. The dynamical behaviour of a moving liquid droplet surrounded by another liquid is dictated by not only the interfacial tension and the droplets viscosity alone, but by the ratio of viscosity between the outer and inner fluids as pointed out by Cox [43]. The problem of moving contact lines in liquid-liquid systems has been studied extensively [44,45]. Yang and co-workers considered the dynamic movement of an L-DEP driven liquid-liquid contact line on a concentric circular electrode in terms of the contact angle [46]. Through experiment and simulations, they demonstrated that the dynamic contact angle of a forced dewetting droplet exponentially approaches the voltage equilibrium contact angle. With the time constant of retraction being proportional to the viscosity η and diameter of the inner droplet D and inversely proportional to the A.C. frequency f i.e. ($\tau \propto D\eta^{0.9}/f^{0.15}$).

3. Applications of dielectrowetting

From an applied perspective, the control over the wettability of a solid surface by a liquid has a wide range of applications, particularly in the fields of microfluidics and optofluidics. Electrowetting on dielectric (EWOD) has become a prominent technology in both fields, however in recent years there has been substantial progress in creating similar devices utilising the dielectrowetting phenomenon. This interest in dielectrowetting based devices has arisen from the restriction of EWOD devices working only with conducting liquids; while dielectrowetting based devices work with any dielectric liquid, this allows the liquid properties, such as refractive index, to be tailored to meet the specific application. Moreover, the contact angle saturation phenomenon with its limitation on the ability of EWOD to spread a droplet into a film can be overcome using a dielectrowetting based approach, opening the way for new thin liquid film based devices. The following section covers some of the applications of dielectrowetting in the field of microfluidics and optofluidics.

3.1. Dielectrowetting in microfluidics

With the demand for smaller and more cost-efficient devices the development of micro-total analysis systems (μ-TAS), more commonly known as Lab on a Chip (LoC) devices, has grown rapidly. LoC devices have the additional benefits of reduced exposure to dangerous pathogens and chemicals along with lowered consumption of reagents. The handling of liquids on the small scale is known as microfluidics which can be broken down into two main categories, continuous microfluidics and discrete or digital microfluidics (DMF). In DMF devices individual droplets are manipulated discreetly, typically through interaction with electric fields. DMF based devices not only overcome the limitations of diffusion based laminar mixing of reagents which is present in continuous microfluidic devices due to low Reynolds number laminar flows; they also offer the ability to have precision control over droplet interactions in a rapid fashion. Several review articles explore the wide field of continuous and discrete microfluidics [47–49•], as such here we shall limit our discussion to the use of dielectrowetting based DMF devices. A thorough review of dielectrowetting in microfluidics is covered in a recent review by Geng and Cho [50].

Jones et al. were the first to demonstrate the potential for L-DEP in microfluidics in 2001 [12]. In their initial work, 100 nL droplets of DI water were dispensed from a large parent droplet which was further broken down into droplets as small as 7 nL. This system was later improved by Jones et al. in which multiple droplets were dispensed through breakup of a longer liquid finger; by tailoring the width and length of the underlying electrode structure the number and volume of the droplets could be tailored to meet a particular need [42]. In this work they also investigated the role of the "droplet dispensing" electrode bumps play in the mechanism concluding that while the dispensing electrodes do not allow the dispensing of droplets at precise

locations, they do contribute to the promotion of the most unstable wavelength [51]. The Jones et al. approach to L-DEP droplet dispensing provides a series of equivolume droplets. Prakash et al. later modified this design to become a tapered electrode structure, allowing the dispensing of droplets of decreasing volume [52]. In 1998, Washizu demonstrated the ability to move droplets of DI water, ionic bio buffers and protein solutions around on a surface using electrostatic forces, where droplets are guided using specially cut grooves into the dielectric layer [53]. The movement of the droplets occurs through the electrostatic lowering of the contact angle on one side of the droplet [54]. Droplets were moved around up to speeds of 400 μm/s with the limiting factor being the speed of the receding contact line. To reduce the actuation voltages and improve transportation speeds Torkkeli and co-workers replaced the hydrophobic layer with a superhydrophobic surface which improved actuation speeds due to the reduced hysteresis of the contact angle [55,56]. While L-DEP based microfluidic devices offer the ability to dispense and manipulate droplets down to the order of picolitres, working with droplets of this size rapid evaporation of the sample becomes a major concern. This is traditionally overcome in microfluidic devices through the use of an ambient oil phase. This oil phase however introduces the complication of sample contamination and perturbations in the flow as pointed out by Prakash & Kaler [57]. They proposed a solution to this using L-DEP to dispense water droplets which were covered in a thin layer of protective oil. By initially dispensing a water droplet and then dispensing a droplet of silicone oil over the water droplet the L-DEP actuation dispenses emulsion droplets on the surface. Ren et al. recently developed a microfluidic pump based on dielectrowetting, where a liquid crystal droplet was actuated within a cavity to exert pressure on a second fluid, which was then dispensed on to a surface [58].

Manipulation of discrete droplets using dielectrowetting was originally suggested by McHale et al. in 2011 [19••] and recently demonstrated by Geng et al. using an embedded linear IDE finger design on six 2 × 2 mm areas combined together using overlapping electrode areas [59••]. This design allows a single droplet to be spread over multiple separately addressable areas at the same time. They demonstrated the splitting of a liquid droplet in a discrete manner through the formation of a liquid finger over 3 addressable areas. By removing the applied voltage to the central area this would cease the L-DEP force in this region thus the droplet would split into two equally sized separate droplets which could then be moved separately over the surface (Fig. 5). Using the same technique droplets of varying size were dispensed from a larger parent droplet. Alongside these advances, they demonstrated this device working with DI water both pure and with a 1% surfactant additive. Actuation of DI water droplets in this manner is something which has not been previously achieved on such an electrode design. This work opens up the possibility for more complex DMF devices based on the dielectrowetting principle providing LoC devices which have only a single active surface.

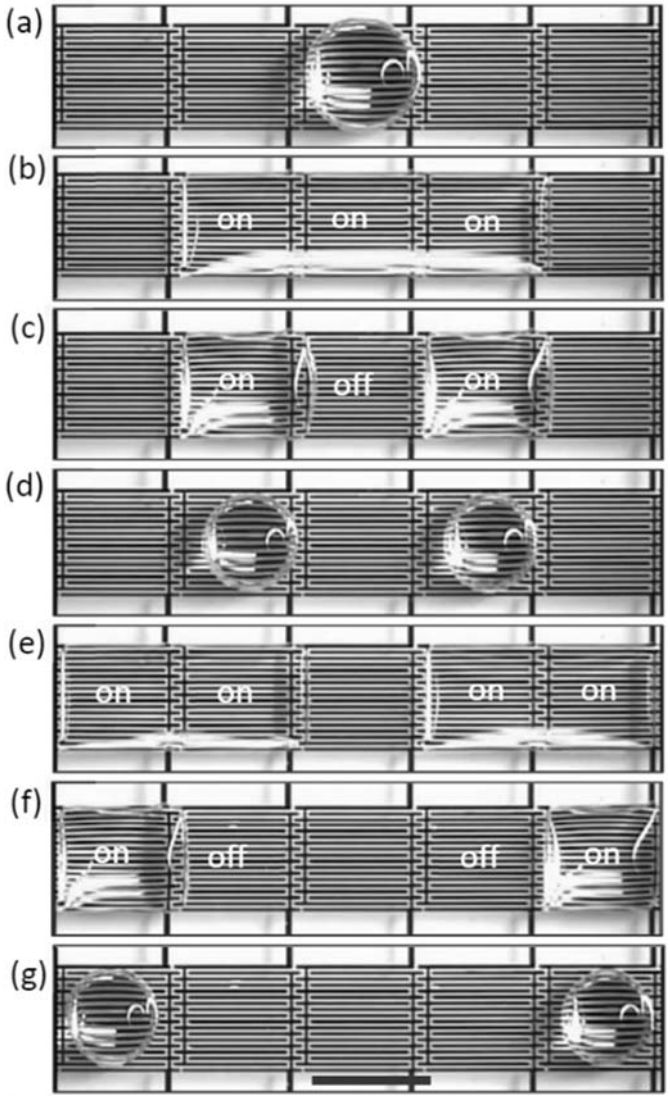

Fig. 5. Splitting and transporting of a propylene carbonate droplet through dielectrowetting (a)–(d) ~2.3 μL droplet split by powering on three adjacent electrode pads then switching off the middle one. (e)–(g) Transporting the split droplets by activating two adjacent pads then switching off the pad opposite to the direction of travel. Scale bar is 2 mm. Reproduced from [59••] with permission of The Royal Society of Chemistry.

3.2. Dielectrowetting driven optical devices

Optofluidic devices manipulate the shape of a liquid interface to modulate the optical properties of the device, such devices offer features such as rapid prototyping, scalability, easy integration and low power consumption. Many optofluidic devices including liquid lenses, irises, shutters and most recently displays have been created utilising interface-localised L-DEP, which can be reinterpreted as the dielectrowetting effect. A thorough review on the use of dielectrowetting in optofluidic devices can be found by Xu et al. [39].

3.2.1. Dielectric liquid lenses

Conventional lenses are made from a solid, typically glass or plastic. While these types of lenses are highly scalable in size they offer no flexibility in terms of optical power due to the fixed focal length. To change the focal length of a lens either a new lens must be cast or a series of lenses combined together which dramatically increases the size of the platform. To meet the focal length switching requirement, liquid lenses have become increasingly popular for small scale applications. The first liquid lens was developed by Cheng et al. [17••] in which a concentric radial electrode design was employed to dielectrowet a liquid crystal droplet in a controllable manner; achieving a focal length change from 1.6 mm to 2.6 mm with the application of 200 V A.C. with switching times of 220 ms while being operated at a maximum power consumption of 1 mW. This work was quickly followed up by Cheng and Yeh in which they developed a liquid lens using the nL-DEP principle, such that a low dielectric droplet acted as the lens the shape of which was controlled by a higher dielectric outer fluid. This reversal allowed the change in focal length to shift from 34 mm to 12 mm while keeping the same power consumption of 1 mW in a fully scalable design [60]. Since this work multiple designs for dielectrowetting driven liquid lenses having varying focal lengths have been developed with reduced power consumption [40,61]. Due to the curvature limitations of single liquid lenses they have an inherent maximum focal length, combining multiple lenses in series allows a much greater range of focal lengths

to be achieved while still keeping the full package smaller than a conventional solid lens system [62]. Zhang et al. recently explored the durability of dielectric liquid lenses to changes in temperature as the properties which define the performance of a liquid lens are temperature dependent quantities. They found that an nL-DEP based liquid lens is thermally stable up to 60 °C with the ability to be heated up to 130 °C and recover its operational capabilities [63]. The flexibility of the lens is also an important consideration as a liquid lens on a curved surface offers a greater field of view and reconfigurability. Lu et al. developed the first dielectrowetting driven flexible liquid lens by patterning the concentric circle electrode design onto a PDMS substrate [64].

3.2.2. Dielectric liquid iris

Another important optical component is the iris, while the mechanical blade version of an iris is relatively inexpensive and highly efficient at blocking unwanted light they are often fragile. Tsai & Yeh developed the first liquid iris based upon the dielectrowetting phenomenon by exploiting the displacement of silicone oil by a propyl alcohol mixed with an opaque ink [65]. This created an iris capable of maintaining a perfectly circular shape while changing its aperture size from 4 mm at 0 V to 1.5 mm at 160 V with a peak power consumption of 5.7 mW. The only drawback to the iris being the reduction in transmittance through the centre of the iris with a 10% reduction in transmitted light intensity. Xu et al. recently demonstrated the capability of their electrode design for lenses in creating a liquid iris capable of changing the aperture from 4.7 mm to 1.2 mm with an actuation of 70 V with scalability for smaller aperture sizes and reduced voltages through changing electrode geometry and higher dielectric constant materials [66].

3.2.3. Dielectrowetting driven gratings

As discussed earlier as the height of a dielectrowetted droplet on a surface approaches the penetration depth of the electric field the liquid-vapor surface becomes distorted by the underlying electric field. Brown and co-workers exploited this effect to create sinusoidal "wrinkles" on the surface of a spread liquid film, where the amplitude of the wrinkles could be dynamically varied by adjusting the applied voltage [18••]. They also showed that as the oil thickness decreases the higher order Fourier components become more evident arising from the charge accumulation at the edges of the electrode fingers.

3.2.4. Dielectrowetting driven optical switches and displays

The use of dielectrowetting in creating optical switches was first pioneered by Ren et al. in 2011, where they utilised a dielectrowetted dyed liquid crystal droplet to block a He-Ne laser beam, with an attenuation of 92% and switching times of 390 and 700 ms on/off respectively [67]. They later followed this work exploring how dielectrowetting could be used to create single pixel colour arrays [68]. Zhao et al. later explored using droplets of dyed propylene glycol on linear IDE structures covered by a Paralyene + Cytop dielectric layer as an optical switch [69]. They demonstrated that up to an 80% attenuation of transmitted light can be achieved at fully spread film state. Following this, they scaled up the design, included a top plate and splitting defects to the design improving the film break up time, with these modifications they obtained switching times of 500 ms on and 1 s off [70]. Lou et al. demonstrated how a quantum dot (QD) display utilising the dielectrowetting shutter mechanism could display 136% of the Adobe RGB colour workspace while maintaining high backlight transmission, greatly improving energy efficiency [71]. More recently, Wang et al. built upon the original Zhao work by miniaturising the device geometry down to 1 mm wide and 0.5 mm tall which enabled switching times to be effectively halved with potential for faster switching times through liquid optimisation [72]. They also demonstrated combining these smaller switches into 2D arrays of a single colour which demonstrate the potential for the development of a dielectrowetting based display.

4. Recent advances in dielectrowetting

4.1. Dielectrowetting on SLIPS

Slippery liquid infused porous (SLIP) surfaces are a recently emerging new type of surface for droplet manipulation. These surfaces are formed from a superhydrophobic porous surface structure which is infused with a liquid, typically silicone oil, which acts to lubricate the contact line of the droplet providing a surface with virtually no hysteresis [73]. Recently Brabcova et al. have demonstrated the ability to perform dielectrowetting on SLIP surfaces [74••]. Using these surfaces, they demonstrated that dielectrowetting (and electrowetting) can be performed with virtually no hysteresis of the contact angle (see Fig. 6). This dramatic reduction in hysteresis should allow droplet movement at much higher speeds than currently possible along with a reduction in both surface biofouling and evaporation due to the thin layer of oil which typically coats droplets. However this new method still requires optimisation as care should be taken with the thickness of the lubricating film as thicker films can retard droplet coalescence as shown by Barman et al. [75].

4.2. Dielectrowetting in manufacturing

While dielectrowetting so far has focused on the reversible manipulation of liquids to create optofluidic and microfluidic devices, these devices have utilised non-volatile liquids. However, if the liquid can become a solid either through heat or exposure to ultra-violet (UV) light, dielectrowetting can be used to control the shape of the final cured solid. This was first pioneered by Wells et al. in 2011 in which they created a solid diffraction grating using UV curable resin with the zeroth order suppressed completely [76•]. Recently, Renaudot et al. manufactured moulds for continuous microfluidic devices by dielectrowetting a UV curable resin into a desired pattern [77]. The advantage of this technique is the removal of the requirement of the photolithographic mask required for SU-8 master mould making which gives the ability to rapidly prototype new devices in less than an hour. In the optofluidic field, Wang and *co*-workers have also demonstrated creating a large area flexible micro-lens array fabricated from cured PDMS on a polyethylene layer in which the focal length was tuneable through the degree of dielectrowetting [78].

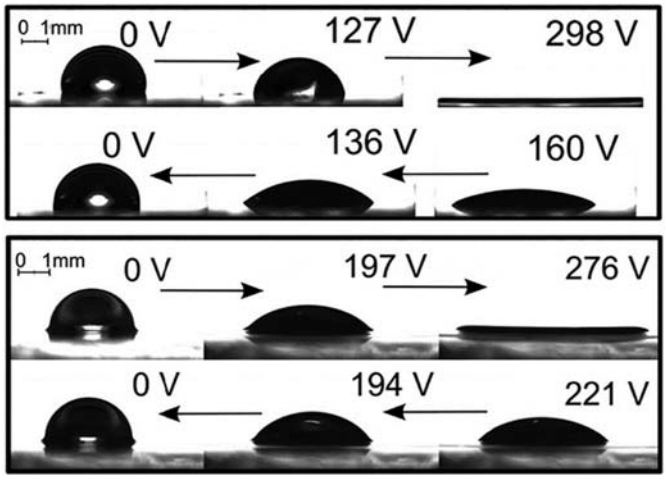

Fig. 6. Side view images of a dielectrowetted glycerol droplet on a spiral electrode design at various rms voltages, during voltage increasing and decreasing cycles while on a normal hydrophobic layer (top), and a SLIPS layer (bottom). Reproduced from [74••], with the permission of AIP Publishing.

4.3. Active control of the cheerios effect

The Cheerios effect is the common phenomenon observed when objects which float on a liquid are attracted or repulsed by each other and the sidewall. This attraction/repulsion is driven by the capillary forces and density disparity between these objects and the sidewall itself [79]. Active control of the Cheerios effect was performed by Yuan and Cho when they demonstrated the ability to modulate the attraction/repulsion by both electrowetting and dielectrowetting [80,81]. Using an interdigitated electrode on a tilted sidewall the contact angle of the dielectric fluid was modified through dielectrowetting, which in turn modulated the attraction/repulsion of a floating object. They investigated the effect of the tilt of the side wall concluding that the optimum tilt angle was 10°. This effect was then utilised to induce the propulsion of a floating object down a small channel through switching of electrode pairs either side of the channel. This method opens up the possibility of controlling the behaviour of particles at interfaces on large scales, promoting self-assembly of monolayers.

4.4. Uses in studying dewetting phenomena

While dielectrowetting has proved vastly useful in creating a variety of microfluidic and optofluidic devices, it also offers the ability to study other more fundamental physical phenomena as demonstrated by Edwards et al. where they have recently used dielectrowetting to provide a deeper understanding of the dewetting mechanism [23•]. By forcing a circular thin film of liquid through dielectrowetting on circular electrodes and then rapidly removing the dielectrowetting component, they studied the evolution of a liquid film dewetting into a single droplet driven purely by capillary forces. This approach removed the assumptions and inertial effects that hinder other methods of studying the phenomena [82,83], allowing them to clearly show that the dewetting of a film into a droplet is not a time reversal of a droplet wetting into a film.

5. Conclusions and outlook

This review has given an overview of the dielectrowetting phenomenon in which the wetting behaviour of non-conducting liquid droplets on solid surfaces can be reversibly modified through an interface localised electric field. The contact angle of the droplet responds following a $\cos(\theta) \propto V^2$ relationship similar to electrowetting but where the ratio of the permittivity of the solid insulator to its thickness is replaced by the ratio of the difference in permittivity of the droplet and immersion fluid to the penetration depth of the electric field. The dielectrowetting approach has been shown to produce a thin liquid film over the complete electrode surface at a critical voltage V_{th}, overcoming the limitations of contact angle saturation present in electrowetting. Since its inception, dielectrowetting has been used to create a variety of microfluidic and optofluidic devices with a positive outlook for the future due to prior limitations of these devices such as non-axisymmetric spreading and large contact angle hysteresis being recently overcome through improved electrode designs and use of a SLIP surface. Future devices are expected to utilize these technological improvements along with higher dielectric liquids to reduce actuation voltages improving the energy consumption and portability of dielectrowetting based devices. One future direction of research into the principles of dielectrowetting is expected to focus on the negative dielectrowetting phenomenon often used in the dielectrowetting based optofluidic devices, as negative dielectrowetting shows deviations away from the expected behaviour for higher voltages.

Acknowledgements

The authors acknowledge G. G. Wells, Z. Brabcova, I. Sage, A. Saxena, R. Ledesma-Aguilar, N. Sampara, C. A. E. Hamlett, N. J. Mottram, A. S. Bhadwal, C. Tsakonas and C. L. Trabi, whose work has contributed to the understanding necessary for this work.

The authors gratefully acknowledge funding for their work provided by the Engineering and Physical Sciences Research Council (EPSRC), U.K., through grants EP/K014803/1, EP/K015192/1, EP/E063489/1.

References and recommended reading•,••

[1] Bonn D, Eggers J, Indekeu J, Meunier J, Rolley E. Wetting and spreading. Rev Mod Phys 2009;81:739–805. https://doi.org/10.1103/RevModPhys.81.739. A comprehensive review covering the statics and dynamics of droplets on surfaces.

[2] Joanny JF, de Gennes PG. A model for contact angle hysteresis. J Chem Phys 1984;81:552–62. https://doi.org/10.1063/1.447337.

[3] Brzoska JB, Azouz IB, Rondelez F. Silanization of solid substrates: a step toward reproducibility. Langmuir 1994;10:4367–73. https://doi.org/10.1021/la00023a072.

[4] Quéré D. Wetting and roughness. Annu Rev Mat Res 2008;38:71–99. https://doi.org/10.1146/annurev.matsci.38.060407.132434.

[5] Zeng J, Korsmeyer T. Principles of droplet electrohydrodynamics for lab-on-a-chip. Lab Chip 2004;4:265–77. https://doi.org/10.1039/b403082f.

[6] Chen L, Bonaccurso E. Electrowetting - from statics to dynamics. Adv Colloid Interface Sci 2014;210:2–12. https://doi.org/10.1016/j.cis.2013.09.007.

[7•] Jones TB, Fowler JD, Chang YS, Kim CJ. Frequency-based relationship of electrowetting and dielectrophoretic liquid microactuation. Langmuir 2003;19:7646–51. https://doi.org/10.1021/la0347511. This paper explores the relationship between electrowetting and L-DEP.

[8] Jones TB, Wang KL, Yao DJ. Frequency-dependent electromechanics of aqueous liquids: electrowetting and dielectrophoresis. Langmuir 2004;20:2813–8. https://doi.org/10.1021/la035982a.

[9••] Mugele F, Baret JC. Electrowetting: from basics to applications. J Phys Condens Matter 2005;17:R705-4. https://doi.org/10.1088/0953-8984/17/28/R01. An excellent review of the field of electrowetting.

[10] Pohl HA. Dielectrophoresis: the behaviour of neutral matter in non-uniform electric fields. Cambridge University Press; 1978.

[11] Jones TB, Perry MP, Melcher JR. Dielectric siphons. Science 1971;174:1232–3. https://doi.org/10.1126/science.174.4015.1232.

[12] Jones TB, Gunji M, Washizu M, Feldman MJ. Dielectrophoretic liquid actuation and nanodroplet formation. J Appl Phys 2001;89:1441–8. https://doi.org/10.1063/1.1332799.

[13•] Jones TB. Liquid dielectrophoresis on the microscale. J Electrostat 2001;51:290–9. https://doi.org/10.1016/S0304-3886(01)00074-2. The first miniturisation of L-DEP electrodes and demonstrates how L-DEP can be used to dispense aqueous droplets.

[14] Chugh D, Kaler KVIS. Leveraging liquid dielectrophoresis for microfluidic applications. Biomed Mater 2008;3:34009. https://doi.org/10.1088/1748-6041/3/3/034009. A comprehensive review of the use of L-DEP in microfluidics for biological applications.

[15] Yi UC, Kim CJ. Characterization of electrowetting actuation on addressable single-side coplanar electrodes. J Micromech Microeng 2006;16:2053–9. https://doi.org/10.1088/0960-1317/16/10/018.

[16] Banpurkar AG, Nichols KP, Mugele F. Electrowetting-based microdrop tensiometer. Langmuir 2008;24:10549–51. https://doi.org/10.1021/la801549p.

[17••] Cheng CC, Alex Chang C, Yeh JA. Variable focus dielectric liquid droplet lens. Opt Express 2006;14:4101. https://doi.org/10.1364/OE.14.004101. This paper presents the first L-DEP based liquid lens.

[18••] Brown CV, Wells GG, Newton MI, McHale G. Voltage-programmable liquid optical interface. Nat Photonics 2009;3:403–5. https://doi.org/10.1038/nphoton.2009.99. The first demonstration of the formation of a thin liquid film on a surface overcoming the contact angle saturation effect.

[19••] McHale G, Brown CV, Newton MI, Wells GG, Sampara N. Dielectrowetting driven spreading of droplets. Phys Rev Lett 2011;107:186101. https://doi.org/10.1103/PhysRevLett.107.186101. This paper demonstrates the concept of interfaced-localised L-DEP and elucidates the relationship between the contact angle and applied voltage.

[20] Brown CV, McHale G, Mottram NJ. Analysis of a static undulation on the surface of a thin dielectric liquid layer formed by dielectrophoresis forces. J Appl Phys 2011;110:24107. https://doi.org/10.1063/1.3606435.

[21] DeGennes PG. Wetting: statics and dynamics. Rev Mod Phys 1985;57:827–63. https://doi.org/10.1103/RevModPhys.57.827.

[22] McHale G, Brown CV, Newton MI, Wells GG, Sampara N. Developing interface localized liquid dielectrophoresis for optical applications. SPIE Proc 2012;8557:855703. https://doi.org/10.1117/12.2001442.

[23•] Edwards AMJ, Ledesma-Aguilar R, Newton MI, Brown CV, McHale G. Not spreading in reverse: the dewetting of a liquid film into a single droplet. Sci Adv 2016;2:e1600183. https://doi.org/10.1126/sciadv.1600183. The first demonstration of how dielectrowetted thin liquid films can be used to study dewetting phenomena.

[24••] McHale G, Brown CV, Sampara N. Voltage-induced spreading and superspreading of liquids. Nat Commun 2013;4:1605. https://doi.org/10.1038/ncomms2619. This paper gives the first study into the dynamics of a dielectrowetted droplet and elucidates the spreading behaviour.

[25] Brown CV, Al-Shabib W, Wells GG, McHale G, Newton MI. Amplitude scaling of a static wrinkle at an oil-air interface created by dielectrophoresis forces. Appl Phys Lett 2010;97. https://doi.org/10.1063/1.3525708.

• of special interest.
•• of outstanding interest.

[26] Wells GG. Voltage programmable liquid optical devices. [Ph.D. Thesis] Nottingham, U.K.: Nottingham Trent University; 2009
[27] Brochard-Wyart F, DeGennes PG. Dewetting of a water film between a solid and a rubber. J Phys Condens Matter 1994;6:A9. https://doi.org/10.1088/0953-8984/6/23A/002.
[28] Fair RB. Digital microfluidics: Is a true lab-on-a-chip possible?, vol. 3; 2007. https://doi.org/10.1007/s10404-007-0161-8.
[29] Jones TB. Dynamics of dielectrophoretic liquid microactuation. Proc 4th int'l conf appl electrost Dalian, China, 8. ; 2001. p. 1–8.
[30] Tanner LH. The spreading of silicone oil drops on horizontal surfaces. J Phys D Appl Phys 1979;12:1473–84. https://doi.org/10.1088/0022-3727/12/9/009.
[31] McHale G, Newton MI, Rowan SM, Banerjee M. The spreading of small viscous stripes of oil. J Phys D Appl Phys 1995;28:1925–9. https://doi.org/10.1088/0022-3727/28/9/020.
[32] McHale G, Shirtcliffe NJ, Aqil S, Perry CC, Newton MI. Topography driven spreading. Phys Rev Lett 2004;93:036102–1. https://doi.org/10.1103/PhysRevLett.93.036102.
[33] Brutin D. Droplet wetting and evapouration. 1st ed. Elsevier; 2015. https://doi.org/10.1007/s13398-014-0173-7.2.
[34] Sampara N. Voltage induced spreading and liquid optical devices. [Ph.D. Thesis] Nottingham, U.K.: Nottingham Trent University; 2013
[35] Yang CC, Yang L, Tsai CG, Jou PH, Yeh JA. Fully developed contact angle change of a droplet in liquid actuated by dielectric force. Appl Phys Lett 2012;101:1–5. https://doi.org/10.1063/1.4759112. An excellent paper exploring the area of negative dielectrowetting, showing how the current theory breaks down at high voltages.
[36] Russell AC, Hsieh WL, Chen KC, Heikenfeld J. Experimental and numerical insights into isotropic spreading and deterministic dewetting of dielectrowetted films. Langmuir 2014;31:637–42. https://doi.org/10.1021/la504066j. The first paper to explore the overcoming of the axisymmetric spreading limitation through the use of a novel electrode design.
[37] Russell A, Kreit E, Heikenfeld J. Scaling dielectrowetting optical shutters to higher resolution: microfluidic and optical implications. Langmuir 2014;30:5357–62. https://doi.org/10.1021/la5008582.
[38] Brabcova Z, McHale G, Wells GG, Brown CV, Newton MI, Edwards AMJ. Near axisymmetric partial wetting using Interface-localized liquid dielectrophoresis. Langmuir 2016;32:10844–50. https://doi.org/10.1021/acs.langmuir.6b03010. A novel 4-phase approach combined with a spiral electrode to overcome the axisymmetric spreading limitation.
[39] Xu S, Ren H, Wu ST. Dielectrophoretically tunable optofluidic devices. J Phys D Appl Phys 2013;46:483001. https://doi.org/10.1088/0022-3727/46/48/483001.
[40] Xu M, Xu D, Ren H, Yoo IS, Wang QH. An adaptive liquid lens with radial interdigitated electrode. J Opt 2014;16:105601. https://doi.org/10.1088/2040-8978/16/10/105601.
[41] Ren H, Xianyu H, Xu S, Wu ST. Adaptive dielectric liquid lens. Opt Express 2008;16:14954–60. https://doi.org/10.1364/OE.16.014954.
[42] Brown CV, McHale G, Trabi CL. Dielectrophoresis-driven spreading of immersed liquid droplets. Langmuir 2015;31:1011–6. https://doi.org/10.1021/la503931p.
[43] Cox RG. The dynamics of the spreading of liquids on a solid surface. Part 1. Viscous flow. J Fluid Mech 1986;168:169. https://doi.org/10.1017/S0022112086000332.
[44] Goossens S, Seveno D, Rioboo R, Vaillant A, Conti J, De Coninck J. Can we predict the spreading of a two-liquid system from the spreading of the corresponding liquid-air systems? Langmuir 2011;27:9866–72. https://doi.org/10.1021/la200439e.
[45] Fetzer R, Ramiasa M, Ralston J. Dynamics of liquid-liquid displacement. Langmuir 2009;25:8069–74. https://doi.org/10.1021/la900584s.
[46] Yang CC, Tsai CWG, Yeh JA. Dynamic behavior of liquid microlenses actuated using dielectric force. J Microelectromech Syst 2011;20:1143–9. https://doi.org/10.1109/JMEMS.2011.2162493.
[47] Samiei E, Tabrizian M, Hoorfar M. A review of digital microfluidics as portable platforms for lab-on a-chip applications. Lab Chip 2016;16:2376–96. https://doi.org/10.1039/C6LC00387G.
[48] Nguyen NT, Hejazian M, Ooi CH, Kashaninejad N. Recent advances and future perspectives on microfluidic liquid handling. Micromachines 2017;8:186. https://doi.org/10.3390/mi8060186.
[49] Berthier J. Microdrops and digital microfluidics. William Andrew; 2008. https://doi.org/10.1016/B978-1-4557-2550-2.00012-2. A comprehensive book exploring both electrowetting and L-DEP based microfluidic devices.
[50] Geng H, Cho SK. Dielectrowetting for digital microfluidics: principle and application. A critical review. Rev Adhes Adhes 2017;5:268–302. https://doi.org/10.7569/RAA.2017.097308.
[51] Ahmed R, Jones TB. Optimized liquid DEP droplet dispensing. J Micromech Microeng 2007;17:1052–8. https://doi.org/10.1088/0960-1317/17/5/027.
[52] Prakash R, Paul R, Kaler KVIS. Liquid DEP actuation and precision dispensing of variable volume droplets. Lab Chip 2010;10:3094–102. https://doi.org/10.1039/c0lc00103a.
[53] Washizu M. Electrostatic actuation of liquid droplets for microreactor applications. IEEE Trans Ind Appl 1998;34:732–7. https://doi.org/10.1109/28.703965.
[54] Pollack MG, Shenderov AD, Fair RB. Electrowetting-based actuation of droplets for integrated microfluidics. Lab Chip 2002;2:96–101. https://doi.org/10.1039/b110474h.
[55] Torkkeli A, Saarilahti J, Haara A, Harma H, Soukka T, Tolonen P. Electrostatic transportation of water droplets on superhydrophobic\nsurfaces. Micro electro mech. syst. 2001. MEMS 2001; 2001. p. 475–8. https://doi.org/10.1109/MEMSYS.2001.906582.
[56] Torkkeli A. Droplets microfluidics on a planar surface. [Ph.D. Thesis] Finland: VTT Technical Research Centre of Finland; 2003. https://doi.org/10.1002/aic.
[57] Prakash R, Kaler KVIS. DEP actuation of emulsion jets and dispensing of sub-nanoliter emulsion droplets. Lab Chip 2009;9:2836–44. https://doi.org/10.1039/b905470g.
[58] Ren H, Xu S, Wu ST. Liquid crystal pump. Lab Chip 2013;13:100–5. https://doi.org/10.1039/C2LC40953D.
[59] Geng H, Feng J, Stabryla LM, Cho SK. Dielectrowetting manipulation for digital microfluidics: creating, transporting, splitting, and merging of droplets. Lab Chip 2017;17:1060–8. https://doi.org/10.1039/C7LC00006E. The first use of dielectrowetting in digital microfluidics, demonstrating all necessary operations.
[60] Cheng CC, Yeh JA. Dielectrically actuated liquid lens. Opt Express 2007;15:7140–5. https://doi.org/10.1364/OE.15.007140.
[61] Xu M, Wang X, Ren H. Tunable focus liquid lens with radial-patterned electrode. Micromachines 2015;6:1157–65. https://doi.org/10.3390/mi6081157.
[62] Li L, Wang D, Liu C, Wang QH. Ultrathin zoom telescopic objective. Opt Express 2016;24:18674–84. https://doi.org/10.1364/OE.24.018674.
[63] Zhang H, Ren H, Xu S, Wu ST. Temperature effects on dielectric liquid lenses. Opt Express 2014;22:1930–9. https://doi.org/10.1364/OE.22.001930.
[64] Lu YS, Tu H, Xu Y, Jiang H. Tunable dielectric liquid lens on flexible substrate. Appl Phys Lett 2013;103:261113. https://doi.org/10.1063/1.4858616.
[65] Tsai CG, Yeh JA. Circular dielectric liquid iris. Opt Lett 2010;35:2484–6. https://doi.org/10.1364/OL.35.002484.
[66] Xu M, Ren H, Lin YH. Electrically actuated liquid iris. Opt Lett 2015;40:831–4. https://doi.org/10.1364/OL.40.000831.
[67] Ren H, Xu S, Wu S-T. Voltage-expandable liquid crystal surface. Lab Chip 2011;11:3426–30. https://doi.org/10.1039/c1lc20367c.
[68] Xu S, Ren H, Liu Y, Wu ST. Color displays based on voltage-stretchable liquid crystal droplet. J Disp Technol 2012;8:336–40. https://doi.org/10.1109/JDT.2012.2186787.
[69] Zhao R, Hua X, Liang Z, Heikenfeld J. Dielectrowetting-based manipulation of droplet and application in light valve. Int. Conf. Opt. Instruments Technol., vol. 9044; 2013; 90440F. https://doi.org/10.1117/12.2036622.
[70] Zhao R, Cumby B, Russell A, Heikenfeld J. Large area and low power dielectrowetting optical shutter with local deterministic fluid film breakup. Appl Phys Lett 2013;103:223510. https://doi.org/10.1063/1.4834095.
[71] Luo Z, Xu S, Gao Y, Lee YH, Liu Y, Wu ST. Quantum dots enhanced liquid displays. J Disp Technol 2014;10:987–90. https://doi.org/10.1109/JDT.2014.2360627.
[72] Wang X, Zhang G, Ren H. Large-area optical switch using surface-expandable liquid droplets. J Disp Technol 2016;12:1565–9. https://doi.org/10.1109/JDT.2016.2567423.
[73] Luo JT, Geraldi NR, Guan JH, McHale G, Wells GG, Fu YQ. Slippery liquid-infused porous surfaces and droplet transportation by surface acoustic waves. Phys Rev Appl 2017;7:14017. https://doi.org/10.1103/PhysRevApplied.7.014017.
[74] Brabcova Z, McHale G, Wells GG, Brown CV, Newton MI. Electric field induced reversible spreading of droplets into films on lubricant impregnated surfaces. Appl Phys Lett 2017;110:121603. https://doi.org/10.1063/1.4978859. This paper represents the first use of a SLIP surface combined with dielectrowetting to overcome the contact angle hysteresis problem when decreasing voltage.
[75] Barman J, Nagarajan AK, Khare K. Controlled electro-coalescence/non-coalescence on lubricating fluid infused slippery surfaces. RSC Adv 2015;5:105524–30. https://doi.org/10.1039/c5ra21936a.
[76] Wells GG, Sampara N, Kriezis EE, Fyson J, Brown CV. Diffraction grating with suppressed zero order fabricated using dielectric forces. Opt Lett 2011;36:4404–6. The first use of a curable material which can be shaped by dielectrowetting before curing into a specific shape.
[77] Renaudot R, Fouillet Y, Jalabert L, Kumemura M, Collard D, Fujita H, et al. Programmable LDEP technology to fabricate versatile master molds for PDMS continuous-flow microfluidic applications. Microfluid Nanofluidics 2014;16:701–10. https://doi.org/10.1007/s10404-013-1256-z.
[78] Wang YC, Tsai YC, Shih WP. Flexible PDMS micro-lens array with programmable focus gradient fabricated by dielectrophoresis force. Microelectron Eng 2011;88:2748–50. https://doi.org/10.1016/j.mee.2011.01.041.
[79] Vella D, Mahadevan L. The cheerios effect. Am J Physiol 2005;73:817–25.
[80] Yuan J, Cho SK. Active control of cheerios effect for dielectric fluid. Proc. IEEE int. conf. micro electro mech. syst; 2015. https://doi.org/10.1109/MEMSYS.2015.7051000.
[81] Yuan J, Feng J, Cho SK. Cheerios effect controlled by electrowetting. Langmuir 2015;31:8502–11. https://doi.org/10.1021/acs.langmuir.5b01479.
[82] Redon C, Brochard-Wyart F, Rondelez F. Dynamics of dewetting. Phys Rev Lett 1991;66:715–8. https://doi.org/10.1016/j.colsurfa.2010.08.006.
[83] Roisman IV, Rioboo R, Tropea C. Normal impact of a liquid drop on a dry surface: model for spreading and receding. Proc R Soc London A Math Phys Eng Sci 2002;458:1411–30. https://doi.org/10.1098/rspa.2001.0923.